XV International Conference on Computational Plasticity. Fundamentals and Applications
COMPLAS 2019
E. Oñate, D.R.J. Owen, D. Peric, M. Chiumenti & Eduardo de Souza Neto (Eds)

A QUASI-STATIC NONLINEAR ANALYSIS FOR ASSESSING THE FIRE RESISTANCE OF 3D FRAMES EXPLOITING TIME-DEPENDENT YIELD SURFACE

D. MAGISANO*, F. LIGUORI*, L. LEONETTI*, D. DE GREGORIO†, G. ZUCCARO† and G. GARCEA*

* Dipartimento di Modellistica per l'Ingegneria
Università della Calabria, 87030 Rende (Cosenza), Italy

† Dipartimento di Strutture per l'Ingegneria e l'Architettura
Università di Napoli Federico II, 801234 Napoli, Italy

Key words: 3D frames, reinforced concrete, yield surface, incremental analysis, fire, fire resistance.

Abstract. In this work an automatic procedure for evaluating the axial force-biaxial bending yield surface of reinforced concrete sections in fire is proposed. It provides an accurate time-dependent expression of the yield condition by a section analysis carried out once and for all, accounting for the strength reduction of the materials, which is a function of the fire duration. The equilibrium state of 3D frames with such yield conditions, once discretized using beam finite elements, is formulated as a nonlinear vectorial equation defining a curve in the hyperspace of the discrete variables and the fire duration. A generalized path-following strategy is proposed for tracing this curve and evaluating, if it exists, the limit fire duration, that is the time of exposure which leads to structural collapse. Compared to the previous proposals on the topic, which are limited to local sectional checks, this work is the first to present a global analysis for assessing the fire resistance of 3D frames, providing a time history of the fire event and taking account of the stress redistribution. Numerical examples are given to illustrate and validate the proposal.

1 Introduction

The evaluation of the carrying capacity of a structure implies not only situations of normal service conditions but also exceptional loadings. An important aspect is to ensure the overall structural integrity during fire events [2]. Usually, frame structures exhibit a relevant overstrength, that is their ultimate capacity can be significantly higher than the elastic limit. For this reason, the material nonlinear analysis is a necessary tool for the structural engineer. A widely employed approach formulates the cross-section yield criterion in terms of generalized stresses, usually axial force and bending moments. For

steel sections, however, the strain limit is sufficiently large to allow the use the classical plasticity theory [19, 11]. A point cloud of generalized yield stresses can be obtained by assigning the corresponding collapse mechanisms, that is the position and orientation of the neutral axis at the collapse states. The Minkowski sum [5] of ellipsoids represents an interesting alternative for the approximation of particular convex shapes known as zonoids, such as the cross-section yield surface [1, 11, 19, 14]. A few ellipsoids can be used to describe the yield surface of homogeneous and composite cross-sections with great accuracy, also in the case of non-smooth shapes. The yield surface at an assigned fire duration can be obtained by simply contracting the ambient temperature yield surface accounting for its strength reduction. The time-dependent yield criteria can be easily used to check the building safety by means of local strength checks of the sections. However, the significant ductility and overstrength of 3D buildings, allow a stress redistribution and can make the sectional check extremely conservative. Although this fact is well known, a global fire analysis accounting for the stress redistribution and the structural overstrength has never been proposed to our knowledge. To deal with the this lack, in this work we propose a quasi-static nonlinear analysis for assessing the global safety of 3D RC frames in conditions of fire. It is a strain-driven incremental strategy which evaluates a sequence of safe states for an increasing fire duration. The time-dependent yield surface together with a finite element beam model allows us to formulate the equilibrium condition of the structure as a nonlinear system of equations defining a curve in the hyperspace of the discrete variables and the fire duration. A generalized path-following strategy is proposed for solving step-by-step the global nonlinear equilibrium equations. The methodology can be seen as an optimisation method [6], which furnishes a sequence of safe states at increasing fire durations according to the lower bound theorem of the limit analysis up to the limit fire duration, that is the time of exposure which leads to the structural collapse. At each step of the analysis the nonlinear internal forces are obtained by an elastic predictor-return mapping process based on the closest point projection (CPP) scheme on the yield surfaces at the current fire duration [16].

2 REINFORCED CONCRETE SECTIONS IN FIRE

In this section, we describe the mechanical model for reinforced concrete sections in fire. In particular, we define the section yield surface in terms of axial force and bending moments corresponding to an assigned fire duration, taking account of the temperature distribution within the section which reduces the strength of the materials.

2.1 Temperature distribution

For a generic solid body with thermal boundary conditions, the heat transfer equations can be solved using the finite element method [10]. For the particular simple case of fire exposed rectangular concrete sections, Wickstrom [21] proposed and validated a set of handy formulas to calculate the 2D temperature distribution. Wickstrom's formulas can be applied for any type of concrete or fire scenario [18]. However, they are particularly easy for ISO 834 standard fire and normal weight concrete.

2.2 Strength reduction for concrete and steel

The concrete compressive strength experiences significant degradation at elevated temperatures. The reduced compressive strength for concretes f_{cT} can be estimated from its ambient value f_c [4] as$f_{cT} = k_c[T]f_c$. Lie et al.'s model [20] is used to predict the reduced yield strength of reinforcing bars f_{yT} from its ambient value f_y as $f_{yT} = k_s[T]f_y$

2.3 Section kinematics and statics

Let us consider a cylinder occupying a reference configuration $\mathcal{B}$ of length ℓ confined by the lateral boundary denoted by $\partial\mathcal{B}$ and two terminal bases Ω_0 and Ω_ℓ. The cylinder is referred to a Cartesian frame $(\mathcal{O}, x_1 \equiv s, x_2, x_3)$ with unit vectors $\{\mathbf{e}_1, \mathbf{e}_2, \mathbf{e}_3\}$ and $\mathbf{e}_1$ aligned with the cylinder axis. In this system, we denote with $\mathbf{X} = s\mathbf{e}_1 + \mathbf{x}$ the position of a point P, where s is an abscissa which identifies the generic cross-section Ω_s of the beam, while $\mathbf{x} = x_2\mathbf{e}_2 + x_3\mathbf{e}_3$ is the position of P inside Ω_s.

The displacement field $\mathbf{u}[\mathbf{X}]$ of the model is expressed, as usual, as a rigid motion of the section

$$\mathbf{u}[\mathbf{X}] = \mathbf{u}_0[s] + \boldsymbol{\varphi}[s] \wedge \mathbf{x} \tag{1}$$

where $\mathbf{u}_0[s]$ and $\boldsymbol{\varphi}[s]$ are the mean translation and rotation of the section and the operator $\wedge$ denotes the cross product. The kinematics assumed in Eq.(1) allows us to evaluate, using a linear Cauchy continuum, the stress-strain work $\mathcal{W}$ in terms of the generalized strains and stresses on the section as

$$\mathcal{W} := \int_\ell (\boldsymbol{\mathcal{N}}[s]^T \boldsymbol{\varepsilon}[s] + \boldsymbol{\mathcal{M}}[s]^T \boldsymbol{\chi}[s]) ds \tag{2}$$

where the generalized strains $\boldsymbol{\varepsilon}$ and $\boldsymbol{\chi}$ are defined as

$$\boldsymbol{\varepsilon}[s] = \mathbf{u}_{0,s}\,[s] + \mathbf{e}_1 \wedge \boldsymbol{\varphi}[s], \quad \boldsymbol{\chi} = \boldsymbol{\varphi}[s]_{,s}\,, \tag{3}$$

a comma stands for derivative and $\boldsymbol{\mathcal{N}}[s] = \{N_1, N_2, N_3\}$ and $\boldsymbol{\mathcal{M}}[s] = \{M_1, M_2, M_3\}$ are the resultant force and moment. Finally, the elastic constitutive law is expressed as

$$\begin{bmatrix} \boldsymbol{\varepsilon} \\ \boldsymbol{\chi} \end{bmatrix} = \mathbf{F} \begin{bmatrix} \boldsymbol{\mathcal{N}} \\ \boldsymbol{\mathcal{M}} \end{bmatrix} \quad , \quad \mathbf{F} = \begin{bmatrix} \mathbf{F}_{NN} & \mathbf{F}_{NM} \\ \mathbf{F}_{NM}^T & \mathbf{F}_{MM} \end{bmatrix} \tag{4}$$

where the coefficients of the cross-section compliance matrix $\mathbf{F}$ can be obtained as in [11, 8].

2.4 The cross-section yield surface

Following [1, 11, 19, 17], we denote with Ω the concrete beam section domain, with A_i the steel rebar area and with (x_{2i}, x_{3i}) its coordinates. The material is assumed to be elastic-perfectly plastic with the plastic admissibility condition expressed in terms of normal stress only as: $-f_{cT} \leq \sigma_{11} \leq 0$ for the concrete and $-f_{yT} \leq \sigma_{11} \leq f_{yT}$ for rebars, where the normal stress is assumed positive in tension. f_{yT} and f_{cT} depend on the value of the temperature T and then from the point coordinates over the section and

fire duration t. Omitting the dependence on s for a clearer exposition, we introduce the plastic mechanism of the cross-section as

$$\mathbf{n} = \{\dot{\epsilon}_1, \dot{\chi}_2, \dot{\chi}_3\} \tag{5}$$

which defines the position and orientation of the neutral axis for the collapse state from the condition

$$\dot{\varepsilon}_{11} \equiv \dot{\epsilon}_1 + x_3\dot{\chi}_2 - x_2\dot{\chi}_3 = 0. \tag{6}$$

The yield stress vector $\boldsymbol{\tau}_y$ collecting the generalized section resultants associated with $\mathbf{n}$ by the Drucker condition, at a given fire duration t, is

$$\boldsymbol{\tau}_y[\mathbf{n}, t] = \begin{bmatrix} N_{y1} \\ M_{y2} \\ M_{y3} \end{bmatrix} \quad \text{with} \quad \begin{cases} N_{y1} = f_y \sum_{i=1}^{N_s} a_i k_s[x_{2i}, x_{3i}, t] A_i - f_c \int_{\Omega_c} k_c[x_2, x_3, t] d\Omega_c \\ M_{y2} = f_y \sum_{i=1}^{N_s} a_i x_{3i} k_s[x_{2i}, x_{3i}, t] A_i - f_c \int_{\Omega_c} x_3 k_c[x_2, x_3, t] d\Omega_c \\ M_{y3} = -f_y \sum_{i=1}^{N_s} a_i x_{2i} k_s[x_{2i}, x_{3i}, t] A_i + f_c \int_{\Omega_c} x_2 k_c[x_2, x_3, t] d\Omega_c \end{cases} \tag{7}$$

where N_s is the number of rebars, Ω_c is the area of the compressed portion of the section according to Eq.(6) and

$$a_i = \text{sign}[\dot{\varepsilon}_{11}[x_{2i}, x_{3i}]]. \tag{8}$$

Equation (7) allows the evaluation, for an assigned fire duration t, of the set of generalized yield stress $\boldsymbol{\tau}_{yk}[t] \equiv \boldsymbol{\tau}_y[\mathbf{n}_k, t]$ associated to the mechanism $\mathbf{n}_k$, simply by assuming uniaxial stress fields reaching their maximum strength capacity in each region, either in tension or in compression.

2.5 Construction of yield surface at ambient temperature as a Minkowski sum of ellipsoids

The domain of the composite cross section $\Omega_s = \Omega \cup_i A_i$ is subdivided into a grid of sub-domains $\Omega_s = \cup_I \Omega_I$. Exploiting the properties of the integral in Eq.(7), the true yield stress $\boldsymbol{\tau}_y[\mathbf{n}_k]$ at ambient temperature can be obtained as

$$\boldsymbol{\tau}_y[\mathbf{n}_k] = \sum_I \boldsymbol{\tau}_{yI}[\mathbf{n}_k] \tag{9}$$

where $\boldsymbol{\tau}_{yI}[\mathbf{n}_k]$ is the contribution of the Ith subdomain evaluated for concrete and of the N_{sI} steel reinforcements belonging to the Ith edge of the section. Equation (9) can be interpreted as a Minkowski sum. Following [14] the stress points on the yield surface expressed as a Minkowski sum of ellipsoids can be parametrized in a closed form in terms of the normal vector $\mathbf{n}$ (see [19]), as

$$\boldsymbol{\tau}[\mathbf{n}] = \sum_I \boldsymbol{\tau}_I[\mathbf{n}] \text{ where } \boldsymbol{\tau}_I[\mathbf{n}] = \mathbf{c}_I + \frac{\mathbf{C}_I \mathbf{n}}{\sqrt{\mathbf{n}^T \mathbf{C}_I \mathbf{n}}}.$$

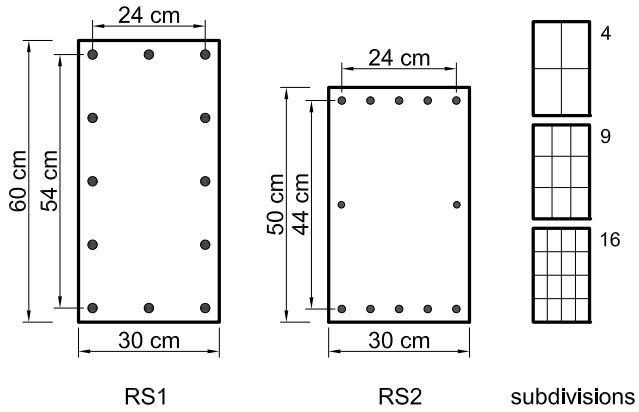

Concrete
$f_{ck} = 20\,MPa$
$\gamma_c = 1.5$
$\sigma_c = f_{ck}/\gamma_c$, $\sigma_t = 0$
Reinforcing bars
$f_{yk} = 450\,MPa$
$\gamma_s = 1.15$
$\sigma_c = \sigma_t = f_{yk}/\gamma_s$
concrete cover $2\,cm$
RS1: $12\phi 20\,mm$
RS2 top and bottom: $10\phi 16\,mm$
RS2 lateral: $2\phi 14\,mm$

Figure 1: Rectangular RC sections: geometry, materials and subdivisions for the geometric Minkowski sum.

2.6 Account of the time-dependent strength reduction

The reduction factors k_c and k_s are functions of the temperature, which depends on the fire duration and on the point (x_2, x_3) within the section, that is we have $k_c[x_2, x_3, t]$ and $k_s[x_2, x_3, t]$. It is possible to evaluate a mean value $\bar{k}_I[t]$ which provides an exact axial force see [16] for details. For the concrete sub-domains, letting $k_I[x_2, x_3, t] = k_c[x_2, x_3, t]$, this means

$$\bar{k}_I[t] = \frac{1}{\Omega_I}\int_{\Omega_I} k_I[x_2, x_3, t]d\Omega_I \;\; \boldsymbol{\tau}[\mathbf{n}, t] = \sum_I \bar{k}_I[t]\boldsymbol{\tau}_I[\mathbf{n}].$$

where the integral can be evaluated analytically as in [3], or numerically using, for instance, the Gauss quadrature.

2.7 Yield surface evaluation of RC sections for beams and columns

The proposed strategy for the evaluation of the time-dependent yield surface is now tested for two RC cross-sections, called $RS1$ and $RS2$, with steel reinforcements of diameter ϕ typical of columns and beams respectively and reported in Fig.1.

The $RS1$ section is analyzed considering a fire exposure all along its perimeter. Figure 2 shows how the proposed Minkowski approximation fits the yield points of the reference solution for different fire durations.

Finally the $RS2$ section is analyzed considering a fire exposure along three edges: left, bottom and right. In Fig.3 we can observe the quality of the proposed Minkowski approximation in fitting the yield points of the reference solution at various fire durations.

3 THE FINITE ELEMENT QUASI-STATIC ANALYSIS FOR 3D FRAMES SUBJECTED TO FIRE

In the following the finite element beam model for the incremental fire analysis is described.

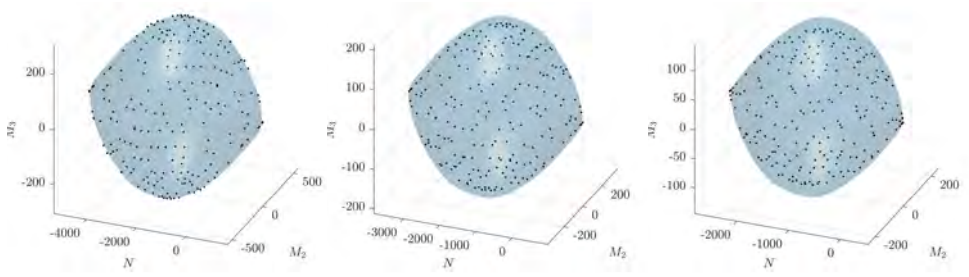

(a) $t = 0$, 2×2 subdomains(b) $t = 1$h, 2×2 subdomains(c) $t = 2$h, 2×2 subdomains

Figure 2: RS1 section: approximation of the true yield points for different fire durations

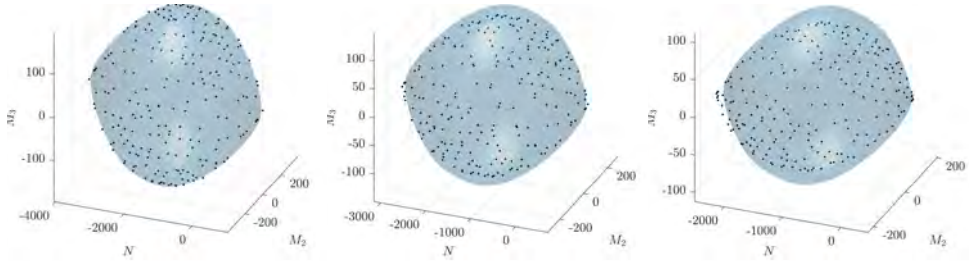

(a) $t = 0$, 2×2 subdomains(b) $t = 1$h, 2×2 subdomains(c) $t = 2$h, 2×2 subdomains

Figure 3: RS2 section: approximation of the true yield points for different fire durations

3.1 THE 3D BEAM FINITE ELEMENT

The beam finite element adopted (see [11]) uses an interpolation of the generalized stresses $[\boldsymbol{\mathcal{N}}, \boldsymbol{\mathcal{M}}]^T = \mathbf{D}_t[s]\boldsymbol{\beta}_e$, where the interpolation matrix $\mathbf{D}_t[s]$ is obtained satisfying the equilibrium equations on the element for zero body forces exactly. Body load effects are then included exactly as a "particular solution". This means that $\boldsymbol{\mathcal{N}}$ and the torsional moment component M_1 are constant, while the two flexural components $M_2[s]$ and $M_3[s]$ of $\boldsymbol{\mathcal{M}}[s]$ are linear with s and linked to the shear resultants so that $N_2\ell = -(M_3[\ell]-M_3[0])$ and $N_3\ell = (M_2[\ell] - M_2[0])$. The internal work becomes

$$\mathcal{W} \equiv \boldsymbol{\mathcal{N}}^T (\mathbf{u}_0[\ell] - \mathbf{u}_0[0]) + \boldsymbol{\mathcal{M}}[\ell]^T\boldsymbol{\varphi}[\ell] - \boldsymbol{\mathcal{M}}[0]^T\boldsymbol{\varphi}[0] = \mathbf{d}_e^T\mathbf{Q}_e^T\boldsymbol{\beta}_e \tag{10}$$

allowing us to directly obtain the discrete form of $\mathcal{W}$ without any FEM interpolation for the kinematic variables. The vectors collecting the kinematics $\mathbf{d}_e$ and static $\boldsymbol{\beta}_e$ finite element generalized parameters and the compatibility operator $\mathbf{Q}_e$ are defined as

$$\boldsymbol{\beta}_e = \begin{bmatrix} N \\ M_2[0] \\ M_3[0] \\ M_2[\ell] \\ M_3[\ell] \\ M_1 \end{bmatrix}, \quad \mathbf{d}_e = \begin{bmatrix} \mathbf{u}_0[0] \\ \boldsymbol{\varphi}[0] \\ \mathbf{u}_0[\ell] \\ \boldsymbol{\varphi}[\ell] \end{bmatrix}, \quad \mathbf{Q}_e = \frac{1}{\ell}\begin{bmatrix} -\ell\,\mathbf{e}_1^T & \mathbf{0} & \ell\,\mathbf{e}_1^T & \mathbf{0} \\ \mathbf{e}_3^T & -\ell\,\mathbf{e}_2^T & -\mathbf{e}_3^T & \mathbf{0} \\ -\mathbf{e}_2^T & -\ell\,\mathbf{e}_3 & \mathbf{e}_2^T & \mathbf{0} \\ -\mathbf{e}_3^T & \mathbf{0} & \mathbf{e}_3^T & \ell\,\mathbf{e}_2^T \\ \mathbf{e}_2^T & \mathbf{0} & -\mathbf{e}_2^T & \ell\,\mathbf{e}_3^T \\ \mathbf{0} & -\ell\,\mathbf{e}_1^T & \mathbf{0} & \ell\,\mathbf{e}_1^T \end{bmatrix}. \tag{11}$$

3.2 The linear elastic problem

The linear elastic problem can be formulated as the stationarity of the Hellinger-Reissner functional Π_{HR} that at the element level can be written as

$$\Pi_{HR} = \mathbf{d}_e^T \mathbf{Q}_e^T \boldsymbol{\beta}_e - \frac{1}{2} \boldsymbol{\beta}_e^T \mathbf{F}_e \boldsymbol{\beta}_e - \mathbf{d}_e^T \mathbf{p}_e$$

where $\mathbf{p}_e$ is the element contribution of the external loads and the elastic compliance matrix of the element $\mathbf{F}_e$ is obtained from the equivalence

$$\int_\ell \left(\begin{bmatrix} \boldsymbol{\mathcal{N}} \\ \boldsymbol{\mathcal{M}} \end{bmatrix}^T \begin{bmatrix} \mathbf{F}_{NN} & \mathbf{F}_{NM} \\ \mathbf{F}_{NM}^T & \mathbf{F}_{MM} \end{bmatrix} \begin{bmatrix} \boldsymbol{\mathcal{N}} \\ \boldsymbol{\mathcal{M}} \end{bmatrix} \right) ds = \boldsymbol{\beta}_e^T \mathbf{F}_e \boldsymbol{\beta}_e, \quad \mathbf{F}_e = \int_\ell \mathbf{D}_t[s]^T \mathbf{F} \mathbf{D}_t[s] \, ds. \tag{12}$$

The stationarity of Π_{HR} with respect to the stress variables furnishes the discrete elastic constitutive law

$$\boldsymbol{\beta}_e[\mathbf{d}_e] = \mathbf{E}_e \mathbf{Q}_e \mathbf{d}_e \quad \text{with} \quad \mathbf{E}_e = \mathbf{F}_e^{-1} \tag{13}$$

which allows us to express the elastic problem in terms of displacement variables only. The stationarity condition with respect to $\mathbf{d}_e$ furnishes the equilibrium equations on the element as

$$\mathbf{Q}_e^T \boldsymbol{\beta}_e[\mathbf{d}_e] - \mathbf{p}_e = \mathbf{0} \tag{14}$$

which, in the elastic case, become

$$\mathbf{K}_e \mathbf{d}_e - \mathbf{p}_e = \mathbf{0} \quad \text{with} \quad \mathbf{K}_e = \mathbf{Q}_e^T \mathbf{E}_e \mathbf{Q}_e.$$

3.3 Stress update for time-dependent yield conditions

An elastic behavior with respect to shear effects as well as torsion is assumed. The section yield function $f[s, t, \boldsymbol{\tau}[s]]$ is then defined in a 3D space involving axial force N_1 and bending moments M_2 and M_3 collected in vector $\boldsymbol{\tau}[s] = \{N_1, M_2, M_3\}$. The plastic admissibility condition on the cross-section s then becomes

$$f[s, t, \boldsymbol{\tau}[s]] \leq 0. \tag{15}$$

The update of the stress is obtained, in a strain-driven way, by means of a closest point projection (CPP) which corresponds to a backward Euler scheme for integrating the constitutive law. Starting from a known state $\mathbf{d}_e[t_0], \boldsymbol{\beta}_e[t_0]$ the stress parameters $\boldsymbol{\beta}_e[\boldsymbol{\beta}_e[t_0], t, \Delta\mathbf{d}_e]$ for an assigned displacement increment $\Delta\mathbf{d}_e$ and a given fire duration t are obtained by solving, for each element, the optimization problem

$$\begin{aligned} &\text{minimize} && \frac{1}{2}(\boldsymbol{\beta}_e - \boldsymbol{\beta}_e^*)^T \mathbf{F}_e (\boldsymbol{\beta}_e - \boldsymbol{\beta}_e^*) \\ &\text{subject to} && f[0, t, \boldsymbol{\tau}[0]] \leq 0 \\ & && f[\ell, t, \boldsymbol{\tau}[\ell]] \leq 0 \end{aligned} \tag{16}$$

where $\boldsymbol{\beta}_e^* = \boldsymbol{\beta}_e[t_0] + \mathbf{E}_e \mathbf{Q}_e \Delta\mathbf{d}_e$ is the elastic predictor and, when the admissibility condition is checked on the beam end nodes only, the generalized normal stress vectors of the two end

sections are extracted directly from $\boldsymbol{\beta}_e$ as $\boldsymbol{\tau}[0] = \mathbf{P}_0\boldsymbol{\beta}_e$ and $\boldsymbol{\tau}[\ell] = \mathbf{P}_\ell\boldsymbol{\beta}_e$ by the extraction operators $\mathbf{P}_0$ and $\mathbf{P}_\ell$. Note that since the mixed finite element always satisfies the local equilibrium, the stresses at both end sections are coupled with each other and, then, the CPP has to be performed at the element level. In this case the element equilibrium equations (14) modify as

$$\mathbf{Q}_e^T\boldsymbol{\beta}_e[\boldsymbol{\beta}_e[t_0], t, \Delta\mathbf{d}_e] - \mathbf{p}_e = \mathbf{0}. \tag{17}$$

A specialized stress update strategy for the Minkowski description of the yield condition can be adopted [14]. The main idea is to reformulate the CPP problem using the normal vector as primal unknown. This is convenient since the dimension of the problem is fixed and independent of the number of ellipsoids used in the approximation. An elastic predictor-return mapping scheme is used. Both the admissibility check and the finite element return mapping are formulated as small nonlinear systems of equations of fixed size.

3.4 Incremental nonlinear fire analysis

Once the finite element assemblage has been carried out, the equilibrium condition of a RC building subjected to fire can be written as

$$\mathbf{r}[\mathbf{d}, t] = \mathbf{s}[\mathbf{d}, t] - \mathbf{p} = \mathbf{0} \tag{18}$$

This system of nonlinear equations represents a curve in the hyperspace $\mathbf{d}$-t, which can be traced in a path-following manner.

The curve can exhibit a limit fire duration, that is the time of exposure which leads to structural collapse. For this reason it is not convenient to use a time controlled scheme since Eq.(18) could not have a solution, that is no equilibrium state, for a given fire duration. We propose instead the use of a generalized arc-length method. The equilibrium equations are completed with the additional constraint $g[\mathbf{d}, t] - \xi = 0$, which defines a surface in $\mathbb{R}^{N+1}$. Assigning successive values to the control parameter $\xi = \xi_{(k)}$ the solution of the nonlinear system

$$\mathbf{R}[\xi] \equiv \begin{bmatrix} \mathbf{r}[\mathbf{d}, t] \\ g[\mathbf{d}, t] - \xi \end{bmatrix} = \mathbf{0} \tag{19}$$

defines a sequence of points (steps) $\mathbf{z}_{(k)} \equiv \{\mathbf{d}_{(k)},\, t_{(k)}\}$ belonging to the equilibrium path. Starting from a known equilibrium point $\mathbf{z}^0 \equiv \mathbf{z}_{(k)}$, the new one $\mathbf{z}_{(k+1)}$ is evaluated correcting a first *extrapolation* $\mathbf{z}^1 = \{\mathbf{d}^1,\, t^1\}$ by a sequence of estimates $\mathbf{z}^j$ by a Newton–Raphson iteration

$$\begin{cases} \mathbf{J}\Delta\mathbf{z} = -\mathbf{R}^j \\ \mathbf{z}^{j+1} = \mathbf{z}^j + \Delta\mathbf{z} \end{cases} \tag{20}$$

where $\mathbf{R}^j \equiv \mathbf{R}[\mathbf{z}^j]$ and $\mathbf{J}$ is the Jacobian of the non-linear system (19) at $\mathbf{z}^j$ or its suitable estimate. The simplest choice for $g[\mathbf{d}, t]$ is the linear constraint corresponding to the

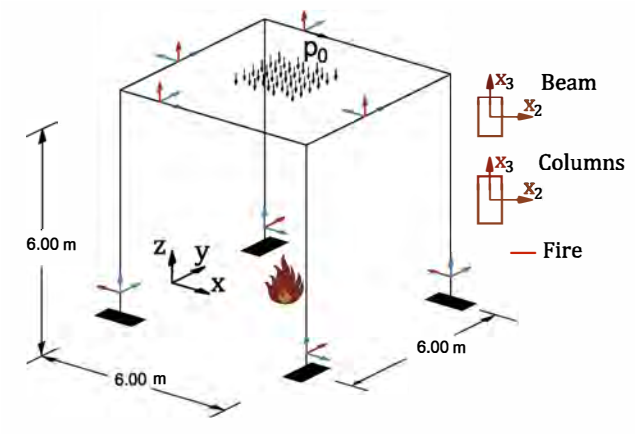

Loads
vertical $p_0 = 15kN/m^2$
Reinforced concrete
Columns section: RS1
Beams section: RS2

Figure 4: Simple 3D frame: geometry, loads and cross-sections

orthogonal hyperplane

$$\mathbf{n}_d^T(\mathbf{d}-\mathbf{d}^j)+n_t\,(t-t^j)=\Delta\xi \quad \text{where} \quad \begin{cases}\mathbf{n}_d \equiv \mathbf{M}\,(\mathbf{d}^j-\mathbf{d}_{(k)})\\ n_t \equiv \mu\,(t^j-t_{(k)})\end{cases} \tag{21}$$

$\mathbf{M}$ and μ being some suitable metric factors [12, 13], $\Delta\xi$ an assigned increment of ξ and

$$\mathbf{J} \equiv \left[\frac{\partial \mathbf{R}[\mathbf{z}]}{\partial \mathbf{z}}\right]_{\mathbf{z}^j} = \begin{bmatrix}\mathbf{K}_t & \mathbf{s}_t\\ \mathbf{n}_d^T & n_t\end{bmatrix}. \tag{22}$$

The time-controlled scheme can be recovered assuming $g[\mathbf{d},t]=t$, but it is not convenient as previously discussed. The solution of Eq.(20) is conveniently performed in a partitioned way as follows

$$\begin{cases}\Delta t = \dfrac{\mathbf{n}_d^T\mathbf{K}_t\mathbf{r}^j}{n_t-\mathbf{n}_d^T\mathbf{K}_t\mathbf{s}_t}\\ \mathbf{K}_t\Delta\mathbf{d}=\Delta t\mathbf{s}_t-\mathbf{r}^j\end{cases} \tag{23}$$

in order to exploit the symmetry and the band structure of the tangent stiffness matrix $\mathbf{K}_t$. The points $\mathbf{z}_{(n)}$ evaluated by the scheme are, by definition, equilibrated and plastically admissible at time $t_{(n)}$. In other words, they satisfy the hypotheses of the lower bound theorem of the limit analysis. Furthermore, in [16], it was proven that when $t_{(n+1)}-t_{(n)}=0$ the structure is just at the point of failure because the hypotheses of the upper and lower bound theorems of the limit analysis are satisfied simultaneously.

4 Numerical test on 3D buildings in fire

The second example regards the simple 3D frame reported in Fig.4. The load over the floor is uniformly distributed over the four beams. The fire scenario considered is the columns exposed to fire at each edge while on the beams it is on the three edges excluding the top one.

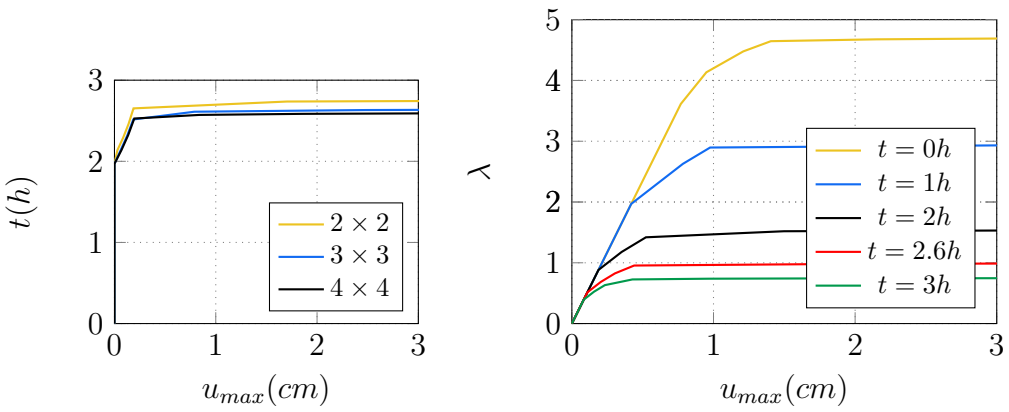

(a) time history (b) evolution for assigned fire durations

Figure 5: Simple 3D frame: equilibrium paths.

In Fig.5 the fire duration-displacement curve for the assigned distributed load is reported. The curve is characterized by a significant inital portion with zero displacements. This means that the load is largely inside the initial domain at ambient temperature. Two hours are required to observe the first plastic deformations while the limit fire duration is equal to 2.6. The structure is analyzed using the standard incremental elasto-plastic analysis with constant yield surfaces corresponding to different fire durations. The load-displacement paths are reported in Fig.5 for different times of exposure. It is possible to observe how the collapse load factor is equal to one for the yield surface corresponding to the limit fire duration evaluated with the proposed incremental strategy.

5 CONCLUSIONS

In this work, we showed a numerical procedure for constructing the axial force-biaxial bending yield surface of sections in fire in a simple, accurate and efficient way. The strategy is based on a particular Minkowski sum of ellipsoids. The yield conditions depends on the fire durations. We proposed a strain-driven incremental strategy for tracing this curve in a path-following quasi-static manner. This kind of analysis takes account of the stress redistribution and provides the limit duration, that is the time of exposure which leads to the structural collapse. The step-by-step procedure furnishes a sequence of safe states at increasing fire durations according to the lower bound theorem of the limit analysis. When a limit fire duration exists, the approach can be framed as an optimisation problem very similar to the static limit analysis one. The main difference is that the loads are kept constant and the fire duration, which leads to a contraction of the yield surfaces, replaces the load factor as objective function. Future developments will focus on accounting for other significant structural behaviors as the effects of large deformations [9].

REFERENCES

[1] Bleyer, J. and De Buhan, P. Yield surface approximation for lower and upper bound yield design of 3D composite frame structures. *Computers and Structures* (2013) **129**:86-98.

[2] Buchanan, Andrew H. and Abu, Anthony K. *Structural design for fire safety.* Wiley, (2017).

[3] El-Fitiany, S.F. and Youssef, M.A. Interaction diagrams for fire-exposed reinforced concrete sections. *Engineering Structures.* (2014) **70**:246-259.

[4] European Union. *EN 1992 - Eurocode 2: Design of concrete structures.* (1992).

[5] Fogel, E. and Halperin, D., E. Exact and efficient construction of Minkowski sums of convex polyhedra with applications. *CAD Computer Aided Design* (2007) **39**:929-940.

[6] Garcea, G. and Leonetti, L. A unified mathematical programming formulation of strain driven and interior point algorithms for shakedown and limit analysis. *Int. J. Num. Meth. Engng.* (2011) **88**:1085-1111.

[7] Garcea, G. and Gonçalves, R. and Bilotta, A. and Manta, D. and Bebiano, R. and Leonetti, L. and Magisano, D. and Camotim, D. Deformation modes of thin-walled members: A comparison between the method of Generalized Eigenvectors and Generalized Beam Theory *Thin-Walled Structures* (2016) **100**:192-212.

[8] Garcea, G. and Gonçalves, R. and Bilotta, A. and Manta, D. and Bebiano, R. and Leonetti, L. and Magisano, D. and Camotim, D. Deformation modes of thin-walled members: A comparison between the method of Generalized Eigenvectors and Generalized Beam Theory *Thin-Walled Structures* (2016) **100**:192-212.

[9] Garcea, G. and Leonetti, L. and Magisano, D. and Gonçalves, R. and Camotim, D. Deformation modes for the post-critical analysis of thin-walled compressed members by a Koiter semi-analytic approach *International Journal of Solids and Structures* (2017) **110-111**:367-384.

[10] Law, A. and Gillie, M. Interaction diagrams for ambient and heated concrete sections *Engineering Structures* (2010) **110-111**:1641 - 1649.

[11] Leonetti, L. and Casciaro, R. and Garcea, G. Effective treatment of complex statical and dynamical load combinations within shakedown analysis of 3D frames *Computers & Structures* (2015) **158**:124 - 139.

[12] Magisano, D. and Leonetti, L. and Garcea, G. How to improve efficiency and robustness of the Newton method in geometrically non-linear structural problem discretized via displacement-based finite elements *Computer Methods in Applied Mechanics and Engineering* (2017) **313**:986-1005.

[13] Magisano, D. and Leonetti, L. and Garcea, G. Advantages of the mixed format in geometrically nonlinear analysis of beams and shells using solid finite elements *Int. J. Num. Meth. Engng.* (2017) **109**:1237-1262.

[14] Magisano, D. and Liguori, F.S. and Leonetti, L. and Garcea, G. Minkowski plasticity in 3D frames: Decoupled construction of the cross-section yield surface and efficient stress update strategy *Int. J. Num. Meth. Engng.* (2018) **116**:435-464.

[15] Magisano, D. and Liguori,F.S. and Leonetti,L. and de Gregorio, D. and Zuccaro, G. and Garcea, G. Minkowski plasticity in 3D frames: A quasi-static nonlinear analysis for assessing the fire resistance of reinforced concrete 3D frames exploiting time-dependent yield surfaces *Computers & Structures* (2019) **212**:327 - 342.

[16] Magisano, D. and Liguori,F.S. and Leonetti,L. and de Gregorio, D. and Zuccaro, G. and Garcea, G. Minkowski plasticity in 3D frames: A quasi-static nonlinear analysis for assessing the fire resistance of reinforced concrete 3D frames exploiting time-dependent yield surfaces *Computers & Structures* (2019) **212**:327 - 342.

[17] Pham, D.T. and de Buhan, P and Florence, C and Heck, J. and Nguyen, H. H. Interaction diagrams of reinforced concrete sections in fire: A yield design approach *Engineering Structures* (2015) **90**:38 - 47.

[18] Del Prete, I. and Cefarelli, G. and Nigro, E. Application of criteria for selecting fire scenarios for structures within fire safety engineering approach *Journal of Building Engineering* (2016) **8**:208 - 217.

[19] Sessa, S. and Marmo, F. and Rosati, L. and Leonetti, L. and Garcea, G. and Casciaro, R. Evaluation of the capacity surfaces of reinforced concrete sections: Eurocode versus a plasticity-based approach *Meccanica* (2018) **6**:1493–1512.

[20] Lie, T.T. Structural fire protection *ASCE manuals and reports on engineering practice* (1992) **78**:241.

[21] Wickstrom, U. A very simple method for estimating temperature in fire exposed concrete structures *Fire Technology Technical report SP-RAPP* (1986) **46**:186-194.